Chapter 3

Cerium Oxides for Corrosion Protection of AZ91D Mg Alloy

Ana Paula Loperena, Ivana Leticia Lehr and Silvana Beatriz Saidman

Additional information is available at the end of the chapter

http://dx.doi.org/10.5772/intechopen.79329

Abstract

Die-cast AZ91D magnesium alloy (8.9 wt.% Al, 0.6 wt.% Zn, 0.2 wt.% Mn, and balance Mg), as novel alternative biodegradable material, has received great attention due to their potential use in biomedical implants. However, their poor corrosion resistance in physiological fluids restricts practical applications. Cerium-based coatings have been studied as an environmental friendly option to enhance the corrosion resistance of magnesium alloys. In order to control the biodegradation rate of AZ91D magnesium alloy in simulated physiological solution, the formation of a coating from a solution containing cerium nitrate ($Ce(NO_3)_3$) was studied. The effect of different additives in the treatment solution (ascorbic acid, citric acid, and sodium citrate) on the anticorrosive properties of the coatings was evaluated. The characterization of the coatings was done using electrochemical techniques and SEM/EDS, XRD, and XPS analyses. The corrosion properties were examined in Ringer solution by polarization studies, open circuit measurements, and faradaic impedance spectroscopy. Results showed that the incorporation of additives improves the anticorrosive properties of the Ce-based film. The coating modified with ascorbic acid provides the best corrosion resistance. According to XPS results, the film is mainly composed by Mg oxides or hydroxides and Ce oxides.

Keywords: cerium oxide, corrosion resistance, AZ91D magnesium alloy, coating, physiological solution

1. Introduction

Magnesium and its alloys are biodegradable and biocompatible materials which exhibit an attractive combination of low density and high strength/weight ratio making them ideal candidates for biomedical applications like substitution and generation of tissues [1]. Temporary

implants of biodegradable materials eliminate the need of a second surgery for implant removal since they are destined to corrode and dissolve postoperatively [2]. However, magnesium-based materials present poor corrosion resistance in physiological environments limiting their applications in the biomedical field. AZ91D magnesium alloy is one of the most commonly used materials, and its corrosion resistance depends on the presence of impure elements acting as active cathode on the microstructure [3].

In order to improve the corrosion resistance of magnesium alloys, some environmentally friendly chemical treatments has been developed [4]. Among them, coatings based on rare earth elements appear as a promising system. Cerium has been studied as alternative to generate protective films. Several researches demonstrated that treatments with cerium salts solutions inhibited the metal corrosion. The formation of cerium oxides and hydroxides on the metal surfaces is generally the reason of this inhibition process because it gives rise to a blocking effect and reduces the rate of reduction reactions [1, 5, 6]. It is known that magnesium alloys oxidation is accompanied with the reduction of hydrogen ions as cathodic reaction. This hydrogen discharge promotes the reaction of Ce^{3+} and Ce^{4+} species with OH^- to form insoluble salts of $Ce(OH)_3$ and $Ce(OH)_4$ due to the increase of the pH in the interface between the substrate and the electrolyte solution [7, 8]. On the other hand, it has been reported that dissolved oxygen can promote the oxidation of Ce^{3+} to Ce^{4+} species. Yu et al. have reported that the cerium precipitation reaction could be affected by the presence of oxygen when the pH solution is in the proper range (pH 4–6) [9]. In addition, Yang et al. demonstrated that the presence of oxygen in the cerium solution promotes the anodic formation of CeO_2 which is better for the formation of compact ceria films [10].

It has been showed that the addition of additives in a cerium solution improves the corrosion resistance of magnesium alloys [11]. Scholes et al. show that the addition of H_2O_2 to the cerium solution is intimated and involved in the deposition process. Hydrogen peroxide acts as oxidant agent and when it is added to the conversion solution, Ce^{3+} ions oxidize to Ce^{4+}. Several studies expose a model of the mechanism by which the cerium-based coatings are formed in the presence of H_2O_2 [12–14]. The addition of hydrogen peroxide in the cerium conversion solution promotes the formation of a cerium hydroxide/oxide coating containing mainly Ce(IV) species which are associated with higher degrees of protection. Chen et al. [15] expose that the concentration of H_2O_2 added to the solution has an important role. In adequate concentrations, H_2O_2 can accelerate the conversion reaction in the formation process; however, if the content of the oxidant exceeds some break value, the coating formed will not be protective for the substrate [6]. In addition, it has been demonstrated that the addition of hydrogen peroxide (H_2O_2) to cerium salts solutions leads to the formation of yellow color coatings due to the presence of Ce(IV). Dabalà et al. report that as the amount of H_2O_2 in the cerium conversion solution increases, more intense yellow color of the coating is obtained on the magnesium alloy surface [6].

With the objective to reduce the velocity of corrosion of AZ91D Mg alloy in physiological simulated solution, the generation of cerium-based coatings on AZ91D Mg alloy was studied in this work. The influence of both the presence of additives in the treatment solution and employed technique on the properties of the coatings was evaluated. Electrochemical and

surface analysis techniques such as SEM, EDS, X-ray diffraction, and X-ray photoelectron spectroscopy (XPS) were employed for characterization of the coatings. The anticorrosive performance of the films was investigated in Ringer solution at 37°C by polarization studies, open circuit measurements, and faradaic impedance spectroscopy.

2. Coating formation

All measurements presented in this chapter were obtained using working electrodes prepared from AZ91D magnesium alloys rods embedded in a Teflon holder with an exposed area of 0.070 cm^2 [16]. The potentials were measured against a saturated Ag/AgCl and a platinum sheet was used as a counter electrode. All chemicals were reagent grade and solutions were made with twice distilled water.

Optimal conversion parameters such as applied potential, pH of the solution, and additives concentrations were determined in order to obtain protective cerium coatings on AZ91D Mg alloy. Potentiodynamic polarization tests in Ringer solution at 37°C were performed to evaluate the corrosion behavior of the electrodes treated in different cerium-based solutions. Thus, the best formation conditions were established.

First, the formation of coating by immersion of AZ91D alloy in a 50 mM $Ce(NO_3)_3$ solution of pH 4.7 at 50°C under open circuit potential conditions was investigated. After 30 min, a discontinuous and not adherent white coating was obtained on the substrate. Different potentials were applied to the working electrode employing the same electrolyte solution in order to check the effects of polarization. **Figure 1** presents the polarization curves in Ringer solution obtained for cerium coatings synthesized at different potentials on AZ91D alloy. The curve for

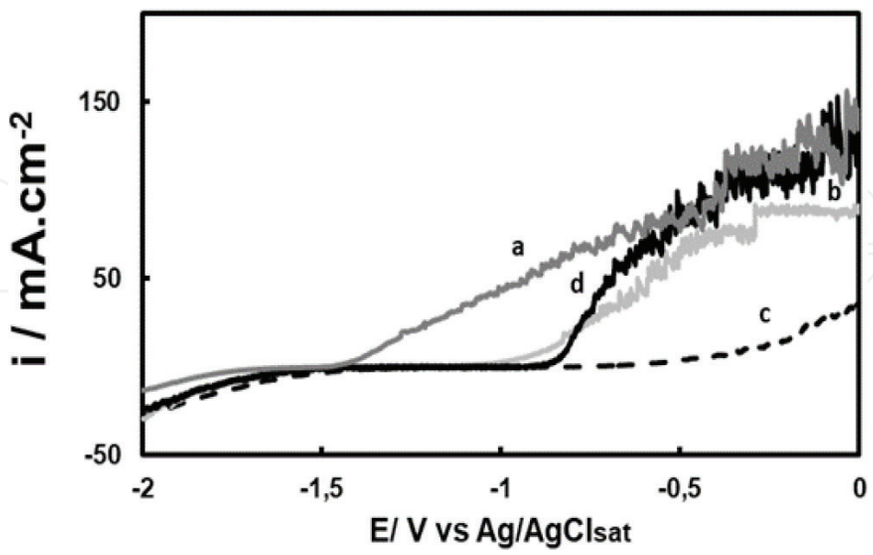

Figure 1. Polarization curves in Ringer solution at 37°C for: (a) AZ91D Mg alloy uncoated and covered with RCe films electrosynthesized in a solution containing 50 mM $Ce(NO_3)_3$ during 30 min at (b) −0.60 V, (c) −0.75 V, and (d) −0.90 V. The scan rate was 0.001 Vs^{-1}.

the bare alloy shows an active dissolution process which starts at −1.478 V (**Figure 1**, curve a). When the substrate is covered by the coating, this process is retarded. The major improvement in corrosion resistance is observed for the film formed at −0.750 V (**Figure 1**, curve c). The corresponding curve exhibits the lowest current densities in the applied potential range. A shift to more positive potentials was also observed indicating that the corrosion reaction of AZ91D alloy is retarded by the presence of the coating. Thus, this potential was selected for further experiments.

Uniform white coatings were obtained on the AZ91D alloy in a 50 mM $Ce(NO_3)_3$ solution at −0.75 V during 30 min. For simplicity purposes this film will be called RCe. It has been demonstrated that the use of additives in the treatment solution could improve the anticorrosive performance of the RCe films [11]. Thus, the effect of the addition of different hydrogen peroxide concentrations (1–20 mM) in the cerium-based baths was evaluated. A more uniform film was formed from the solution containing 50 mM $Ce(NO_3)_3$, 6 mM H_2O_2, and pH 3.6. This additive produces the oxidation of Ce^{3+} to Ce^{4+} favoring the incorporation of cerium(IV) in the film [15]. A yellow coating is observed on the substrate after the potentiostatic formation. This coating will be called RCe-H_2O_2. According to the literature, cerium(IV) is responsible of the appearance of the yellow coating [17], while the presence of Ce_2O_3 or $Ce(OH)_3$ is related to the white color.

It is known that both Mg and Al are immediately oxidized during immersing of AZ91D alloy in a solution containing $Ce(NO_3)_3$ and H_2O_2. The stable species of Mg in solutions with pH value less than 8.5 is Mg^{2+} while in the case of aluminum is Al^{3+} for solutions with pH value less than 4 [18]. Proton, oxygen, and H_2O_2 reductions can occur simultaneously with the oxidation of the substrate. Based on the experimental conditions of our work, H_2O_2 is the main oxidizing agent, in accordance with the proposition of Yu et al. [9]. Moreover, the addition of H_2O_2 to the treatment solution is necessary for the development of a yellowed coating which is associated with the presence Ce^{4+} species. As was mentioned above, H_2O_2 is a strong oxidizing agent, and its presence in the cerium solution can promote the oxidation which accelerates the precipitation of the conversion coating. On the other hand and, as was stated, the presence of H_2O_2 can produce the oxidation of Ce(III) to Ce(IV). Ce(III) and Ce(IV) species react with OH^- to form insoluble salts of $Ce(OH)_3$ and $Ce(OH)_4$ as film components. As the pH in the interface between the substrate and the solution increases as a result of the hydrogen discharge, the precipitation reaction is favored. On the other hand, it has been informed that when H_2O_2 concentration is around 80 mg/L, an increase in the deposition rate of insoluble salts occurs, and in effect, a porous coating is formed on the substrate surface [15]. Thus, the incorporation of a proper amount of H_2O_2 in the treatment bath improves the corrosion performance of Ce-based film on AZ91D alloys.

Polarization curves for the bare alloy and alloy covered with cerium-based coatings are presented in **Figure 2**. In comparison with RCe, a considerable potential shift to more positive values is observed for RCe-H_2O_2. Thus, the addition of oxidant in the cerium-based bath enhances the corrosion performance of RCe coating.

In order to improve the corrosion resistance of the cerium-based coating obtained in the presence of H_2O_2, different additives were evaluated. Thus, the inhibition effect of three additives

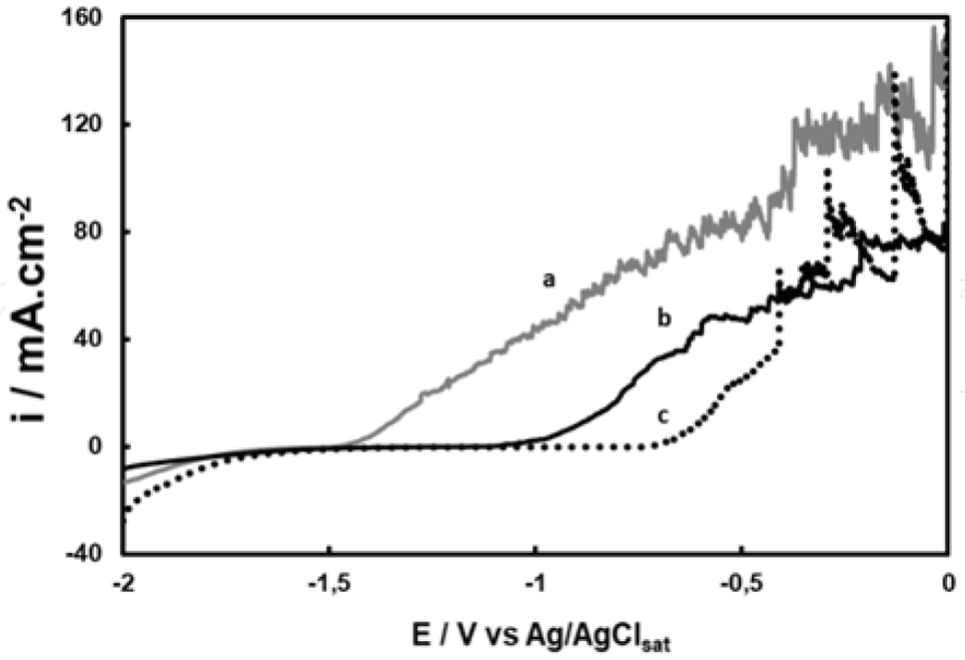

Figure 2. Polarization behavior in Ringer solution at 37°C for: (a) AZ91D Mg alloy, (b) RCe coating, and (c) RCe-H_2O_2 coating. The scan rate was 0.001 Vs^{-1}.

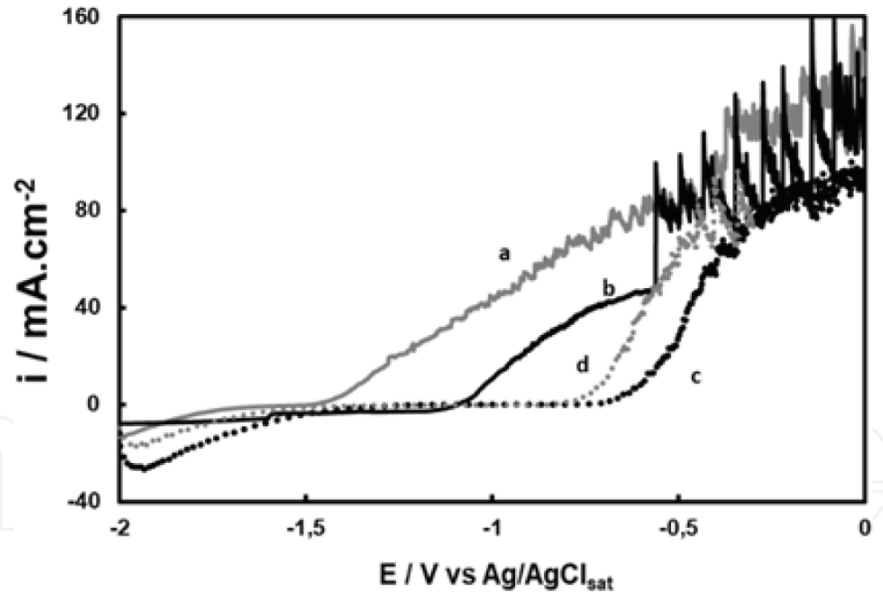

Figure 3. Polarization behavior for AZ91D alloy at 37°C in Ringer solution containing different H_3Cit concentrations: (a) 0 mM, (b) 5 mM, (c) 10 mM, and (d) 15 mM. The scan rate was 0.001 Vs^{-1}.

(citric acid (H_3Cit), ascorbic acid (Hasc), and sodium citrate (Na citrate)) on the electrochemical response of bare AZ91D alloy in Ringer solution was studied. For each additive a range of concentrations was evaluated in order to establish the best conditions to be used in Ce film formation. **Figures 3–5** show the polarization curves of AZ91D magnesium alloy in Ringer solutions containing different additive concentrations. It can be observed that the degradation

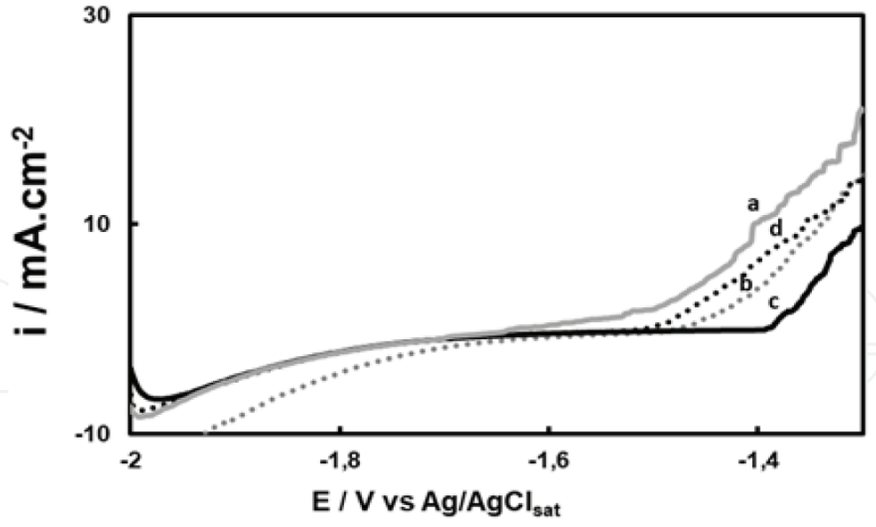

Figure 4. Polarization behavior for AZ91D alloy at 37°C in Ringer solution containing different HAsc concentrations: (a) 0 mM, (b) 1 mM, (c) 5 mM, and (d) 10 mM. The scan rate was 0.001 Vs^{-1}.

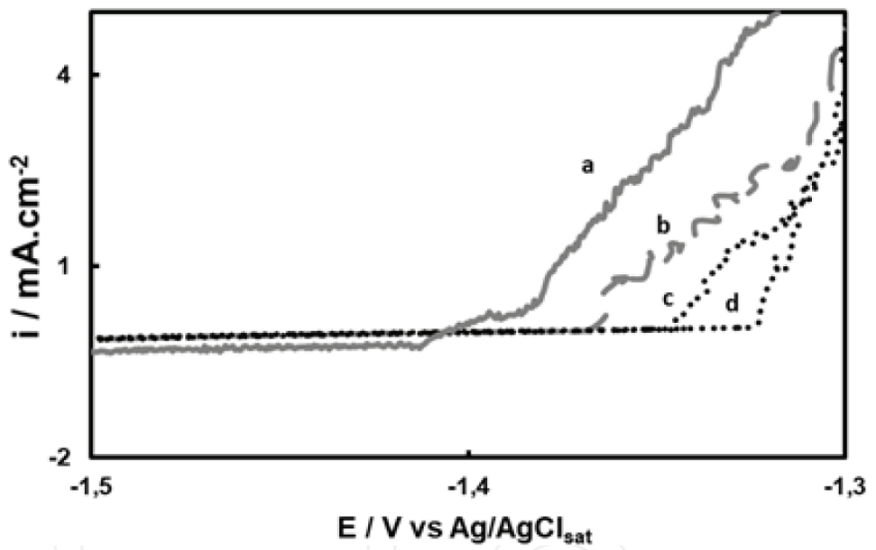

Figure 5. Polarization behavior for AZ91D alloy at 37°C in Ringer solution containing different Na citrate concentrations: (a) 0 mM, (b) 1 mM, (c) 5 mM, and (d) 15 mM. The scan rate was 0.001 Vs^{-1}.

rate of AZ91D alloy is retarded by the presence of the H_3Cit at concentrations up to 10 mM (**Figure 1**, curve c), while the effect is opposite for higher concentrations (**Figure 3**, curve d). Thus, the best inhibitive performance was obtained for 10 mM H_3Cit. A similar procedure was carried out in order to analyze HAsc (**Figure 4**) and Na citrate (**Figure 5**), respectively. The optimum concentration of HAsc was 5 mM (**Figure 4**, curve b), while for Na citrate the best inhibitor effect was obtained for 15 mM (**Figure 5**, curve c).

It is known that compounds with functional groups containing oxygen act as effective corrosion inhibitors for metallic materials in aqueous chloride solution by a surface complex formation [19]. Also, it is known that a chelating agent should have two opposite effects on

the corrosion of metals and may act as either an inhibitor or corrosive [20]. With respect to the effects of H_3Cit, Wang reported that a cerium conversion coating on AZ91 magnesium alloy formed from ethanol solution containing $Ce(NO_3)_3$ and citric acid showed good corrosion performance [17]. The authors postulated that Mg ions originated from the dissolution of the alloy during immersion in the treatment bath reacted with Cit^{3-} and partly deposited on the alloy surface in the form of Mg_3Cit_2 that is insoluble in ethanol. According to the theory of chemical adsorption of organic inhibitors, the chelating agent which forms a stable and insoluble chelate with a metal in certain medium can inhibit corrosion. HAsc is a well-known inhibitor for several metallic materials. The inhibitor character of HAsc has been extensively studied for steel in acid and neutral media [21–23]. Valek et al. reported that the generation of a protective oxide film on steel is associated with the formation of an insoluble surface chelate at an optimal concentration of 10^{-3} M [23]. However, these authors also informed that the formation of a soluble chelate has a stimulatory action in Fe dissolution at concentrations above 5×10^{-3} M. It has been informed that HAsc presents a dual role, in some conditions it can act as corrosion inhibitor, and in other cases, it can increase the corrosion rate of stainless steel (SS)X_4Cr_{13} in HCl solutions [24]. At the present time the inhibition effect of HAsc on the corrosion of magnesium alloys has not been reported. The results obtained here are in accordance with the tendency informed in the bibliography for other metallic materials. So, for an optimal HAsc concentration (5 mM), the precipitation of an insoluble surface chelate confers protection to the magnesium alloy through the formation of a physical barrier. On the other hand, for a HAsc concentration above 5 mM, the degradation rate of AZ91D alloy increases due to the formation of soluble chelates.

It has been demonstrated that sodium citrate can act as brightening, leveling, and buffering agent in electrodeposition electrolytes and, thus, eliminates the need for other additives [25]. Moreover, it is mainly known as a complexing agent. Organic compounds with carboxylate group have been presented as promising corrosion inhibitors of carbon steel in high-alkaline-media-containing chloride ions [26–29]. In addition, citrate ions were presented as good pitting inhibitors, as they could adsorb on the carbon steel (without a passive layer), avoiding chloride ions adsorption due to a steric effect [28]. It has been reported that citrate ions present a chelating effect, forming soluble complexes with Fe(II) and Fe(III) [30]. Bahramian et al. show that sodium citrate proved to be an effective and economical additive to improve the properties of Ni-P coatings obtained on Cu substrate; its impact depended only slightly on its concentration [31]. The effect of Na citrate as corrosion inhibitor in chloride solution was studied for AZ31D and AM60 Mg alloys [32, 33]. It has been demonstrated that Na citrate forms chelates with Mg^{2+}. Although the chelate is soluble, it can be absorbed on the surface of the substrate by the oxygen atom, hindering the adsorption of Cl^- [33].

From the corrosion inhibition behavior shown above, the optimal concentration of each additive for coating formation was selected. Thus, the treatment solutions contain 50 mM $Ce(NO_3)_3$, 6 mM H_2O_2, and:

- 10 mM H_3Cit. This film will be called RCe-H_3Cit.
- 5 mM HAsc. This film will be called RCe-HAsc.
- 15 mM Na citrate. This film will be called RCe-citrate.

In all cases, a golden-yellow-colored coating was observed with the naked eyes when the substrate was polarized at −0.75 V during 30 min in the treatment solution at 50°C.

3. Evaluation of the anticorrosive properties of the coatings

Polarization measurements in Ringer solution were carried out in order to study the corrosion behavior of the coating formed in the presence of additives (**Figure 6**). A positive potential shift and the low current density measured indicate a better corrosion resistance of the coated samples. In the case of the RCe-HAsc film, a significative increase in the anodic current can be observed at more anodic potential values (**Figure 6**, curve d). It can also be noted that the addition of H_3Cit or Na citrate in the treatment solution does not improve the anticorrosive performance of RCe-H_2O_2 coatings.

Based on the above results, we decided to only study the anticorrosive performance of RCe-H_2O_2 and RCe-HAsc coatings. First, it is important to mention that the RCe coating was very adherent and could be removed only by mechanical polishing. Adherence force of RCe-H_2O_2 and RCe-HAsc was 34.3 and 43.4 N, respectively. Thus, adhesion of the films increases when the additive is added to the treatment solution.

To evaluate the degree of corrosion protection attained after covering the substrate, the variation of the open circuit potential (OCP) as a function of time was carried out in Ringer solution (**Figure 7**). Uncoated sample reaches the pitting potential (−1.503 V) after approximately 5 h of immersion (**Figure 7**, curve a). The electrode covered with the coating obtained without the additive reached the corrosion potential of the uncoated AZ91D alloy after 36 h of immersion (**Figure 7**, curve b). In the case of the coating generated in the presence of the HAsc, at the beginning, the OCP value was −1.320 V (**Figure 7**, curve c). Then, the OCP reached −1.150 V

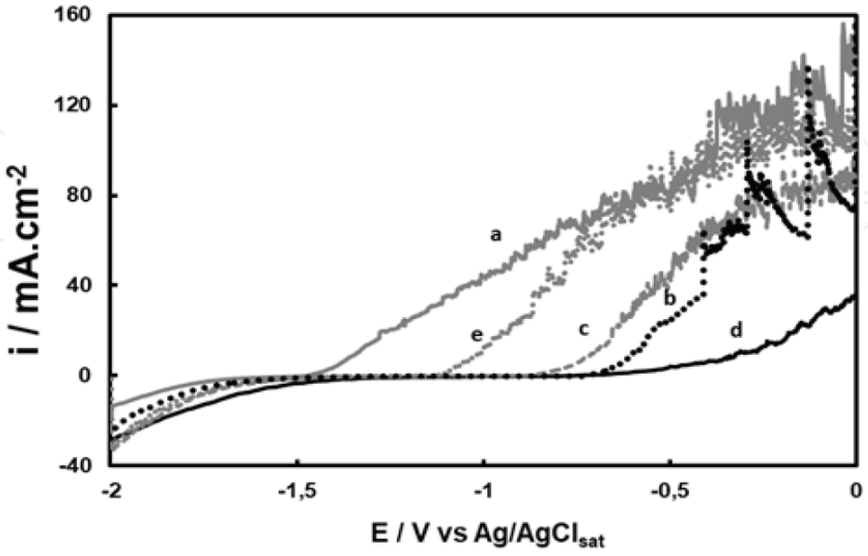

Figure 6. Polarization behavior in Ringer solution at 37°C for: (a) uncoated AZ91D alloy, (b) RCe-H_2O_2 coating, (c) RCe-H_3Cit coating, (d) RCe-HAsc coating, and (e) RCe-citrate coating. The scan rate was 0.001 Vs^{-1}.

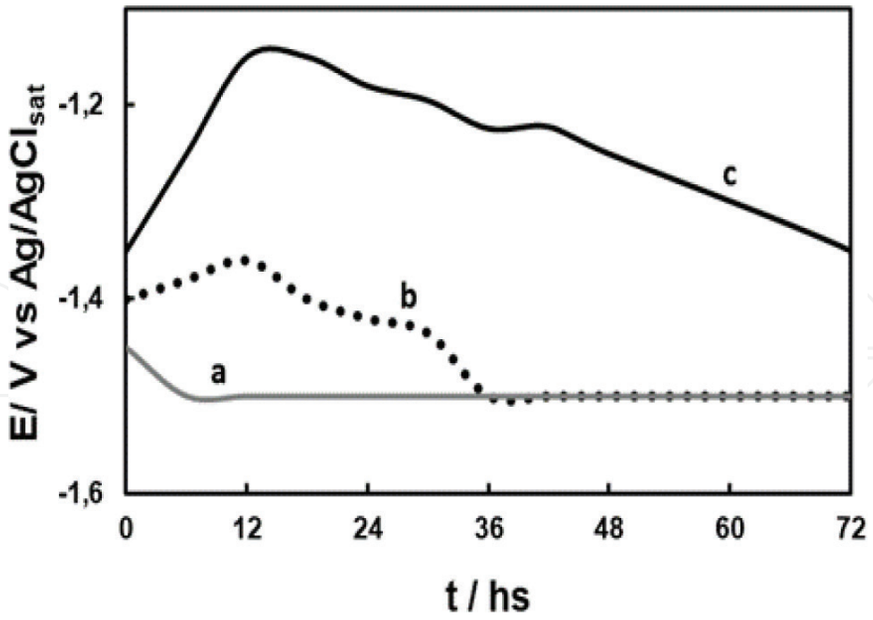

Figure 7. Time dependence of the OCP in Ringer solution for: (a) AZ91D magnesium alloy, (b) RCe-H_2O_2 film, and (c) RCe-HAsc coating.

and kept the same value during 18 h. The OCP was approximately −1.350 V after 72 h of immersion. This potential value was still nobler than that for the uncoated electrode.

Figure 8 shows the Tafel polarization plots for uncoated and coated AZ91D alloy. Estimation of the corrosion parameters (E_{corr}, cathodic (B_c) and anodic (B_a) Tafel slopes and corrosion current (i_{corr})) is reported in **Table 1** for RCe-H_2O_2 and RCe-HASc coatings. The i_{corr} values measured for the coatings are lower than that for the bare AZ91D alloy. In the case of treated samples, the i_{corr} value is one order of magnitude lower than that of the uncoated substrate. However, higher displacement of E_{corr} to more noble potentials was obtained for the RCe-HAsc film compared to RCe-H_2O_2 coating (**Table 1**).

To obtain more information about the anticorrosion protection of RCe-H_2O_2 and RCe-HAsc film, EIS measurements were conducted in Ringer solution (**Figure 9**). For comparison, the impedance response of uncoated substrate was also presented in **Figure 9**, curve a. Two capacitive loops and one inductive loop were observed in the Nyquist diagram of the AZ91D Mg alloy as was observed for other magnesium alloys [34]. It has been postulated that relaxation processes of adsorbed species ($Mg(OH)^+$ or $Mg(OH)_2$) on the surface of untreated alloys/pure Mg leads to an inductive response at low frequencies [35]. After 5 min of immersion, the impedance response for the coated electrodes exhibit two capacitive loops in the high- and low-frequency ranges. It is known that the diameter of the capacitive loops is associated with the charge-transfer resistance (R_{ct}) and therefore with the corrosion resistance. The R_{ct} values for RCe-HAsc coating are much larger than that of RCe-H_2O_2 film indicating a better corrosion protection.

The performance of the RCe-HAsc at different immersion times in Ringer solution was analyzed by Nyquist plots (**Figure 10**). After 6 h of immersion, all the impedance diagrams

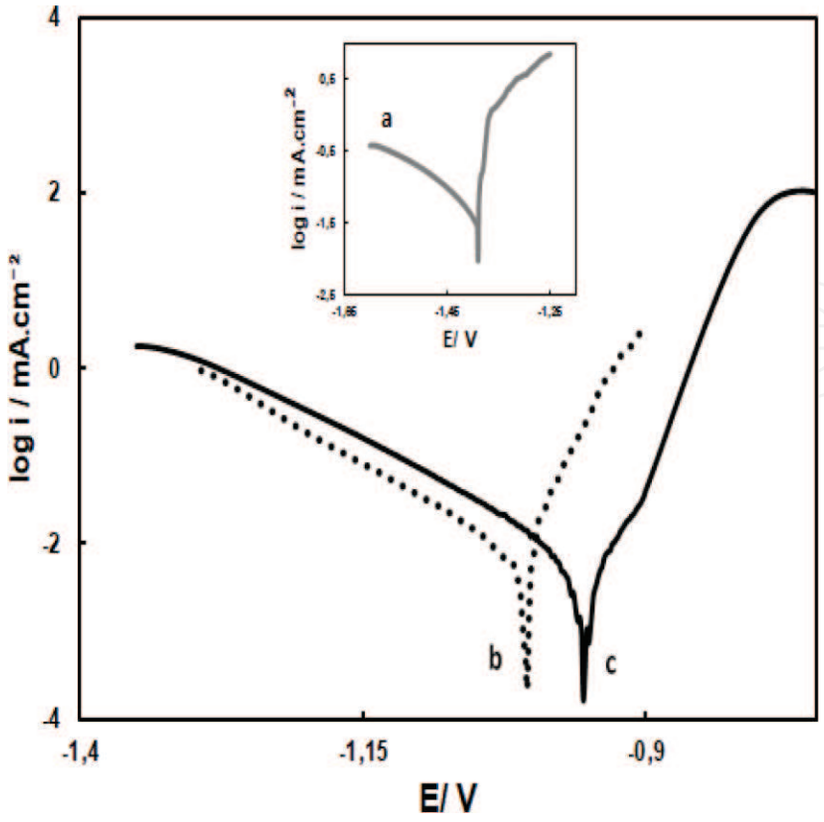

Figure 8. Tafel curves obtained in Ringer solution at 37°C for: (a) uncoated AZ91D alloy, (b) RCe-H_2O_2, and (c) RCe-HAsc. The scan rate was 0.001 Vs^{-1}.

	E_{corr}/V	i_{corr}/mAcm^{-2}	B_a/V	B_c/V
AZ91D	−1.501 ± 0.050	0.1050 ± 0.0050	0.045	−0.293
RCe-H_2O_2	−1.002 ± 0.020	0.0057 ± 0.0002	0.034	−0.122
RCe-HAsc	−0.952 ± 0.015	0.0054 ± 0.0002	0.032	−0.126

The mean values and their standard deviation are presented.

Table 1. Corrosion parameters estimated from Tafel polarization plots for uncoated AZ91D, RCe-H_2O_2, and RCe-HAsc formed on AZ91D alloy.

exhibit a capacitive loop in the high- and medium-frequency ranges. As can be observed, the diameter of capacitive loop increases gradually with increasing time until 36 h, indicating an improvement in the anticorrosion performance of the coating with time. This result corroborates that the RCe-HAsc can effectively improve the corrosion resistance of the alloy.

In order to confirm the improvement in the corrosion protection of the AZ91D alloy imparted by the RCe-HAsc film, the quantity of Mg released in Ringer solutions after 5 h of immersion under open circuit potential conditions was determined. When the substrate was covered with the RCe-HAsc coating, the amount of Mg released was 2.01 mg/L and for the uncoated sample the value was 3.90 mg/L. So the corrosion rate is nearly twice less for the sample coated by the RCe-HAsc film. This result confirms a good performance of the RCe-HAsc coating even after a long exposure time.

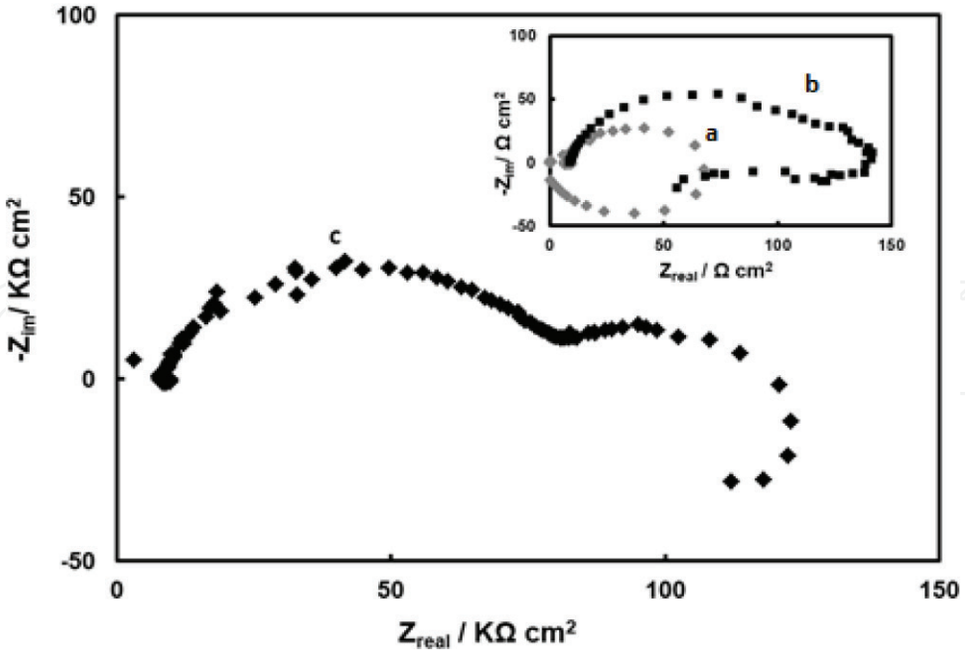

Figure 9. Nyquist plots of the impedance spectra obtained at OCP conditions after 5 min of immersion in Ringer solution at 37°C for: (a) AZ91D Mg alloy, (b) RCe-H_2O_2 film, and (c) RCe-HAsc film.

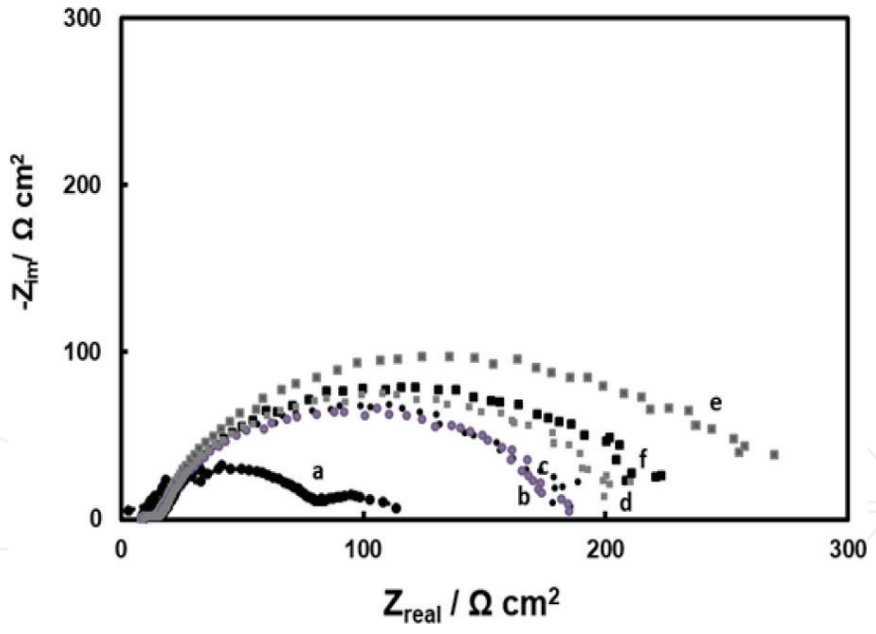

Figure 10. Nyquist plots of the impedance spectra obtained at OCP conditions in Ringer solutions at 37°C for RCe-HAsc coating, after different immersion times: (a) 5 min, (b) 6 h, (c) 12 h, (d) 24 h, (e) 36 h, and (f) 48 h.

When the uncoated AZ91D alloy is immersed in simulated physiological solution, it suffers significant degradation. As mentioned above, it is proposed that the general corrosion mechanism of Mg alloys implies Mg oxidation to Mg^{2+} with simultaneous water reduction. Cathodic reactions lead to a local alkalization which produces $Mg(OH)_2$ precipitation [36, 37]. The β-phase acts as the cathode and α-phase acts as the anode. The active surface area is reduced by RCe-HAsc film, and in consequence, less area of the substrate is available to be corroded. The potential difference

between α- and β-phases becomes smaller when the AZ91D alloy is coated by an adherent and stable film. Thus, the micro-galvanic couple effect is reduced [38, 39]. In summary, the coating confers a physical barrier between the substrate and the corrosive medium. In addition, the improvement in the corrosion resistance is associated with the presence of insoluble precipitates of cerium and the inhibitor effect of ascorbic acid. As mentioned previously, the HAsc has inhibition ability by insoluble chelates formation and it is responsible for the increased corrosion protection of RCe films. The presence of HAsc decreases the dissolution rate of the substrate during the coating formation allowing the formation of a more compact and protective film.

4. Morphological and compositional characterization of RCe-HAsc coating

Figure 11 presents the SEM image of the film obtained in solution containing 50 mM Ce $(NO_3)_3$ + 6 mM H_2O_2 (**Figure 11A**) or 50 mM $Ce(NO_3)_3$ + 6 mM H_2O_2 + 5 mM HAsc (**Figure 11B**). A cracked mud morphology is observed of RCe film. The dehydration of the surface film after the deposition leads to crack formation [40]. It has been suggested that the formation of gas bubbles on the substrate, combined with a dehydration process or also with shearing stresses between the alloys and the obtained film, is responsible of the cracked structure [41].

A more uniform and compact film with the presence of only some microcracks was obtained by the addition of HAsc in the conversion solution. From the SEM cross-sectional micrography, the thickness of the RCe-HAsc coating is approximately 5 μm (**Figure 12**).

The presence of cerium in the coating was confirmed by EDX analysis (**Figure 13**). It is known that RCe coatings are obtained from the precipitation of oxides, due to an increase in local pH at the interface substrate/solution.

Figure 14 presents the XRD patterns of the AZ91D alloy and treated samples. By comparison it can be concluded that the coatings are composed of CeO_2, Ce_2O_3, and $Mg(OH)_2$.

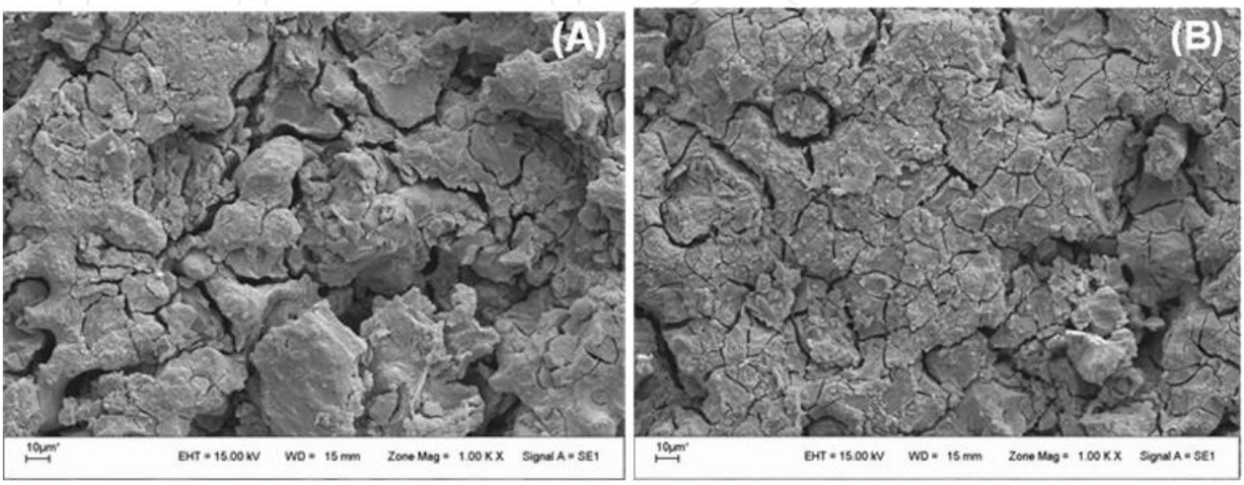

Figure 11. SEM image of the films obtained on AZ91D alloy. The film was formed at - 0.75 V during 30 min in 50 mM $Ce(NO_3)_3$ and 6 mM H_2O_2: (A) without HAsc and (B) with 5 mM HAsc.

http://dx.doi.org/10.5772/intechopen.79329

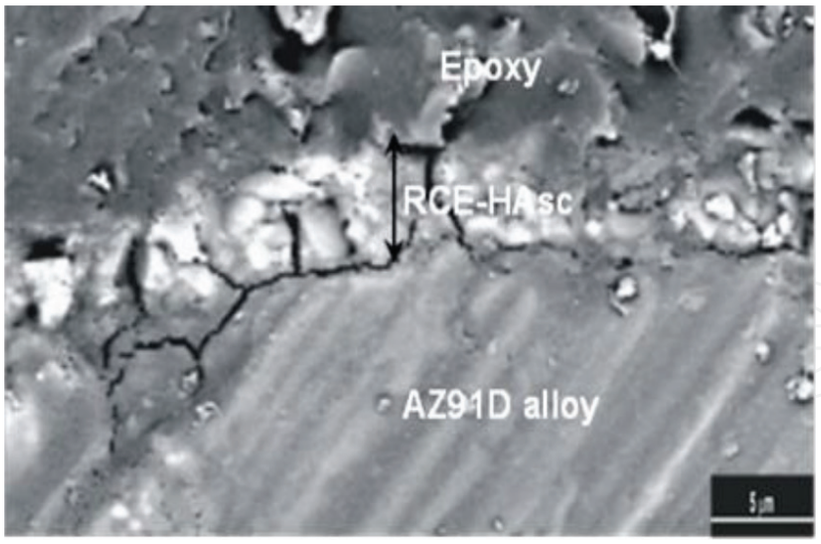

Figure 12. SEM micrograph showing the cross-section of RCe-HAsc coating. The coating was electrosynthesized at −0.75 V during 30 min in a solution containing 50 mM $Ce(NO_3)_3$, 6 mM H_2O_2, and 5 mM HAsc.

In order to determine the surface chemical composition of RCe-HAsc coating, the XPS was employed. The XPS results are shown in **Figure 15**.

The main components are magnesium, oxygen, and cerium. **Figure 16** shows the XPS analysis of the specific electron binding energies of Mg, O, and Ce elements. From the Mg 2p spectrum, presented in **Figure 15**, it can be determined that Mg in the coating is present as MgO and $Mg(OH)_2$ [2].

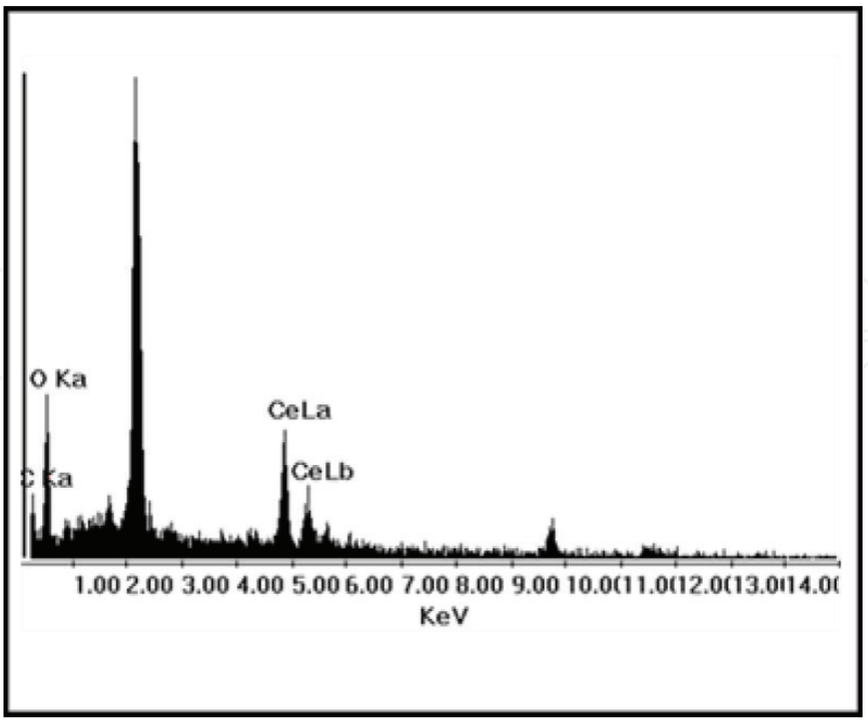

Figure 13. EDS spectrum of RCe-HAsc coating formed on AZ91D alloy. The coating was electrosynthesized at −0.75 V during 30 min in a solution containing 50 mM $Ce(NO_3)_3$, 6 mM H_2O_2, and 5 mM HAsc.

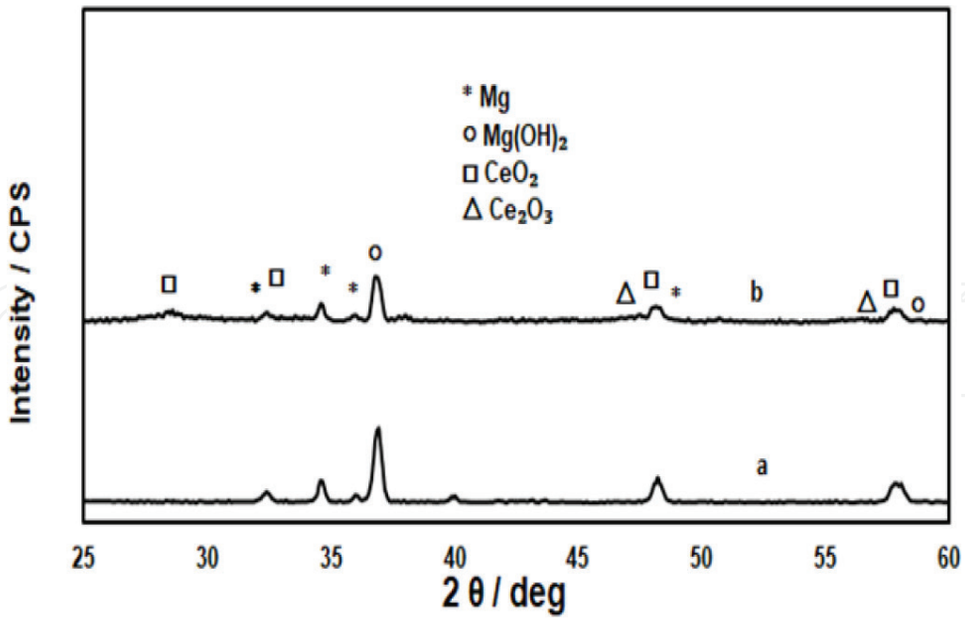

Figure 14. XRD spectra for: (a) AZ91D alloy and (b) RCe-HAsc coating.

Figure 16B shows the spectrum of O 1 s. The peak at 531.25 eV is attributed to metallic oxides [2]. The Ce $3d_{5/2}$ and Ce $3d_{3/2}$ peaks are presented in **Figure 16C**. The analysis established that the binding energies at 916.0, 897.89, and 880.90 eV correspond to CeO_2, CeO, and Ce_2O_3, respectively. The satellite peak around 916.0 eV confirms the presence of Ce(IV) ions in the coating. The ratio between Ce(IV) and Ce(III) was 1.503. In summary, from the XPS results, it was concluded that the RCe-HAsc film is mainly composed of CeO_2, CeO, Ce_2O_3, MgO, and $Mg(OH)_2$.

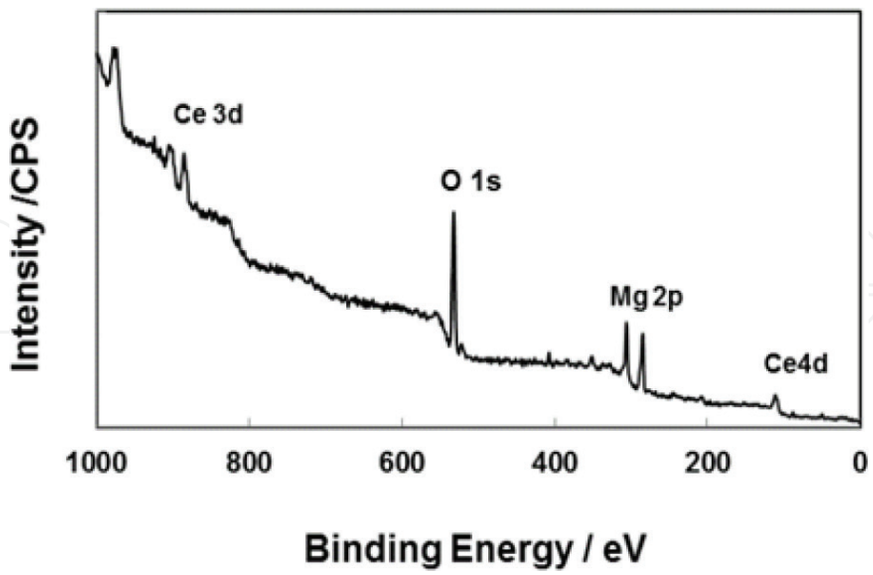

Figure 15. XPS survey spectrum of RCe-HAsc coating formed on AZ91D alloy. The coating was electrosynthesized at −0.75 V during 30 min in 50 mM $Ce(NO_3)_3$, 6 mM H_2O_2, and 5 mM HAsc.

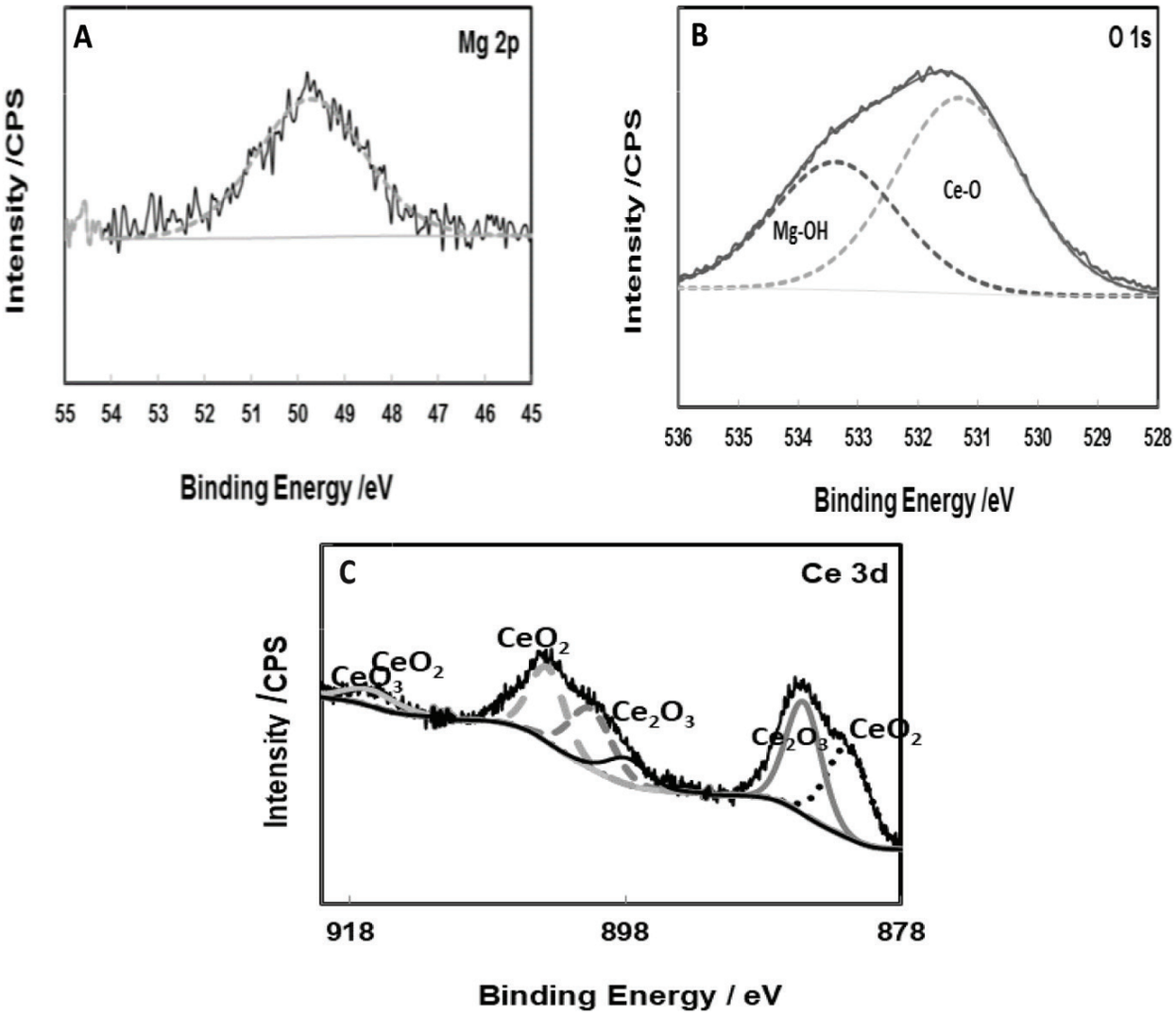

Figure 16. XPS intensities of: (A) Mg 2p, (B) O 1 s, and (C) Ce 3d. The coating was electrosynthesized at −0.75 V during 30 min in 50 mM $Ce(NO_3)_3$, 6 mM H_2O_2, and 5 mM HAsc.

5. Conclusions

Adherent and uniform cerium-based coatings were obtained on AZ91D magnesium alloy in solutions containing cerium nitrate, H_2O_2, and three different additives (H_3Cit, HAsc, and Na-citrate). The most adherent films were obtained by a potentiostatic polarization at −0.75 V. The RCe-HAsc-coated AZ91D alloy exhibited better corrosion resistance in Ringer solution. Magnesium oxides or hydroxides and cerium oxides are the main components of the film. The anticorrosive properties of RCe-HAsc film in simulated body fluid solution is superior to those of films formed in the absence of HAsc. The improvement in the corrosion resistance is associated with the presence of insoluble precipitates of cerium and the effect of the additive through the formation of insoluble chelates.

Acknowledgements

CONICET, ANPCYT, and Universidad Nacional del Sur, Bahía Blanca, Argentina, are acknowledged for financial support.

Nomenclature

EDX	energy dispersive X-ray spectroscopy
EIS	electrochemical impedance spectroscopy
HAsc	ascorbic acid
H_3Cit	citric acid
Na-citrate	sodium citrate
RCe	cerium-based coating obtained at −0.75 V in 50 mM $Ce(NO_3)_3$ solution
RCe-H_2O_2	cerium-based coating obtained at −0.75 V in 50 mM $Ce(NO_3)_3$ and 6 mM H_2O_2 containing solution
RCe-HAsc	cerium-based coating obtained at −0.75 V in 50 mM $Ce(NO_3)_3$, 6 mM H_2O_2, and 5 mM HAsc containing solution
SEM	scanning electron microscopy
XPS	X-ray photoelectron spectroscopy
XRD	X-ray powder diffraction

Author details

Ana Paula Loperena, Ivana Leticia Lehr* and Silvana Beatriz Saidman

*Address all correspondence to: ilehr@uns.edu.ar

Chemical Engineering Department, Institute of Electrochemical and Corrosion Engineering, National University of the South, Bahía Blanca, Argentina

References

[1] Rudd AL, Breslin CB, Mansfeld F. The corrosion protection afforded by rare earth conversion coatings applied to magnesium. Corrosion Science. 2000;**42**:275-288. DOI: 10.1016/S0010-938X(99)00076-1

[2] Zheng YF, Gu XN, Witte F. Biodegradable metals. Materials Science and Engineering R. 2014;**77**:1-34. DOI: 10.1016/j.mser.2014.01.001

[3] Ballerini G, Bardi U, Bignucolo R, Ceraolo G. About some corrosion mechanisms of AZ91D magnesium alloy. Corrosion Science. 2005;**47**:2173-2184. DOI: 10.1016/j.corsci.2004.09.018

[4] Hornberger H, Virtanen S, Boccaccini AR. Biomedical coatings on magnesium alloys—A review. Acta Biomateralia. 2012;**8**:2442-2455. DOI: 10.1016/j.actbio.2012.04.012

[5] Montemor MF, Simoes AM, Ferreira MGS, Carmezim MJ. Composition and corrosion resistance of cerium conversion films on the AZ31 magnesium alloy and its relation to the salt anion. Applied Surface Science. 2008;**254**:1806-1814. DOI: 10.1016/j.apsusc.2007.07.187

[6] Dabalà M, Brunellia K, Napolitanib E, Magrinia M. Cerium-based chemical conversion coating on AZ63 magnesium alloy. Surface and Coatings Technology. 2003;**172**:227-232. DOI: 10.1016/S0257-8972(03)00336-0

[7] Yasakau KA, Zheludkevich ML, Lamaka SV, Ferreira MGS. Mechanism of corrosion inhibition of AA2024 by rare-earth compounds. Journal of Physical Chemistry B. 2006;**110**:5515-5528. DOI: 10.1021/jp0560664

[8] Castano C, O'Keefe M, Fahrenholtz W. Cerium-based oxide coatings. Current Opinion in Solid State and Materials Science. 2015;**19**:69-76

[9] Yu P, Hayes SA, O'Keefe TJ, O'Keefe MJ, Stoffer JO. The phase stability of cerium species in aqueous systems II. The Ce III/IV-H_2O-H_2O_2/O_2 systems. Equilibrium considerations and Pourbaix. Diagram calculations. Journal of the Electrochemical Society. 2006;**153**:C74-C79. DOI: 0013-4651/2005/1531/C74/6

[10] Yang Y, Yang Y, Du X, Chen Y, Zhang Z, Zhang J. Influences of the main anodic electroplating parameters on cerium oxide films. Applied Surface Science. 2014;**305**:330-336. DOI: 10.1016/j.apsusc.2014.03.078

[11] Cui X, Yang Y, Liu E, Jin G, Zhong J, Li Q. Corrosion behaviors in physiological solution of cerium conversion coatings on AZ31 magnesium alloy. Applied Surface Science. 2011;**257**:9703-9709. DOI: 10.1016/j.apsusc.2011.04.141

[12] Scholes MF, Soste C, Hughes AE, Hardin SG, Curtis PR. The role of hydrogen peroxide in the deposition of cerium-based conversion coatings. Applied Surface Science. 2006;**253**:1770-1780. DOI: 10.1016/j.apsusc.2006.03.010

[13] Valdez B, Kiyota S, Stoytcheva M, Zlatev R, Bastidas JM. Cerium-based conversion coatings to improve the corrosion resistance of aluminium alloy 6061-T6. Corrosion Science. 2014;**87**:141-149. DOI: 10.1016/j.corsci.2014.06.023

[14] Eslamia M, Fedela M, Speranzab G, Defloriana F, Anderssonc N, Zanellac C. Study of selective deposition mechanism of cerium-based conversion coating on Rheo-HPDC aluminium-silicon alloys. Electrochimica Acta. 2017;**255**:449-462. DOI: 10.1016/j.electacta.2017.09.182

[15] Chen S, Zhang S, Ren X, Xu S, Yin L. Cerium-based chemical conversion coating on aluminum alloy to inhibits corrosion in chloride solution. International Journal of Electrochemical Science. 2015;**10**:9073-9088

[16] Loperena P, Lehr I, Saidman S. Formation of a cerium conversion coating on magnesium alloy using ascorbic acid as additive. Characterisation and anticorrosive properties of the formed films. Journal of Magnesium and Alloys. 2017;**4**:278-285. DOI: 10.1016/j.jma.2016.10.002

[17] Wang C, Zhu S, Jiang F, Wang F. Cerium conversion coatings for AZ91D magnesium alloy in ethanol solution and its corrosion resistance. Corrosion Science. 2009;**51**: 2916-2923. DOI: 10.1016/j.corsci.2009.08.003

[18] Zhou W, Shan D, Han E, Wei K. Structure and formation mechanism of phosphate conversion coating on die-cast AZ91D magnesium alloy. Corrosion Science. 2008;**50**: 329-337. DOI: 10.1016/j.corsci.2007.08.007

[19] Kuznetsov YI, Thomas JGN, Mercer AD. Organic Inhibitors of Corrosion of Metals. New York: Springer Science & Business Media; 1996. 284 p. DOI: 10.1007/978-1-4899-1956-4

[20] Katoh M. Influence of chelating agent (citric acid) and F− on corrosion of Al. Corrosion Science. 1968;**8**:423-431. DOI: 10.1016/S0010-938X(68)90084-X

[21] Ferrerira ES, Giacomellu C, Spinelli A. Evaluation of the inhibitor effect of L-ascorbic acid on the corrosion of mild steel. Materials Chemistry and Physics. 2004;**83**:129-134. DOI: 10.1016/j.matchemphys.2003.09.020

[22] Akrout H, Bousselmi L, Triki E, Maximovitch S, Dalard F. Effect of non-toxic corrosion inhibitors on steel in chloride solution. Journal of Materials Science. 2004;**39**:7341-7350. DOI: 10.1023/B:JMSC.0000048749.31437.b9

[23] Valek L, Martinez S, Mikulic D, Brnardic I. The inhibition activity of ascorbic acid towards corrosion of steel in alkaline media containing chloride ions. Corrosion Science. 2008;**50**:2705-2709. DOI: 10.1016/j.corsci.2008.06.018

[24] Fuchs-Godex R, Pavlovic M, Tomic M. The inhibitive effect of vitamin-C on the corrosive performance of steel in HCl solutions. International Journal of Electrochemical Science. 2013;**8**:1511-1519

[25] Orinákova R, Turonová A, Kladeková D, Gálová M, Smith RM. Recent developments in the electrodeposition of nickel and some nickel-based alloys. Journal of Applied Electrochemistry. 2006;**36**:57-972. DOI: 10.1007/S10800-006-9162-7

[26] Muralidharan S, Saraswathy V, Thangavel K, Srinivasan S. Competitive role of inhibitive and aggressive ions in the corrosion of steel in concrete. Journal of Applied Electrochemistry. 2000;**30**:1255-1259. DOI: 10.1023/A:1026570120698

[27] Muralidharan S, Saraswathy V, Nima SPM, Palaniswamy N. Evaluation of a composite corrosion inhibiting admixtures and its performance in Portland Pozzolana cement. Materials Chemistry and Physics. 2004;**86**:298-306. DOI: 10.1016/j.matchemphys.2004.03.025

[28] Ormellese M, Lazzari L, Goidanich S, Fumagalli G, Brenna A. A study of organic substances as inhibitors for chloride-induced corrosion in concrete. Corrosion Science. 2009;**51**:2959-2968. DOI: 10.1016/j.corsci.2009.08.018

[29] Martinez S, Valek L, Oslakovic IS. Adsorption of organic anions on low-carbon steel in saturated $Ca(OH)_2$ and the HSAB principle. Journal of the Electrochemical Society. 2007;**154**(11):C671-C677. DOI: 10.1149/1.2777882

[30] Vino A, Shweky I, Cohen S, Bauminger ER, Lippard SJ. A novel nonairon(III) citrate complex: A ferric triple-decker. Inorganic Chemistry. 1998;**37**(20):5168-5172. DOI: 10.1021/ic9715658

[31] Bahramian A, Eyraud M, Vacandio F, Knauth P. Improving the corrosion properties of amorphous Ni-P thin films using different additives. Surface and Coatings Technology. 2018;**345**:40-52. DOI: 10.1016/j.surfcoat.2018.03.075

[32] Dai Y, Li Q, Gao H, Li LQ, Chen FN, Luo F, et al. Effects of five additives on electrochemical corrosion behaviours of AZ31D magnesium alloy in sodium chloride solution. Surface Engineering. 2011;**27**(7):536-543. DOI: 10.1179/1743294410Y.0000000025

[33] Liu D, Song Y, Sha D, Han E-H. Comparison of the inhibition effect of four inhibitors on the corrosion behavior of AM60 magnesium alloy. International Journal of Electrochemical Science. 2018;**13**:2219-2235. DOI: 10.20964/2018.03.23

[34] Srinivasan A, Blawert C, Huang Y, Mendis CL, Kainer KU, Hort N. Corrosion behavior of Mg-Gd-Zn based alloys in aqueous NaCl solution. Journal of Magnesium and Alloys. 2014;**2**:245-256. DOI: 10.1016/j.jma.2014.08.002

[35] Anik M, Celikten G. Analysis of the electrochemical reaction behavior of alloy AZ91 by EIS technique in H_3PO_4/KOH buffered K_2SO_4 solutions. Corrosion Science. 2007;**49**:1878-1894. DOI: 10.1016/j.corsci.2006.10.016

[36] Zhang Y, Yan C, Wang F, Li W. Electrochemical behavior of anodized Mg alloy AZ91D in chloride containing aqueous solution. Corrosion Science. 2005;**47**:2816-2831. DOI: 10.1016/j.corsci.2005.01.010

[37] Pardo A, Merino MC, Coy AE, Arrabal R, Viejo F, Matykina E. Corrosion behavior of magnesium/aluminum alloys in 3.5 wt.% NaCl. Corrosion Science. 2008;**50**:823-834. DOI: 10.1016/j.corsci.2007.11.005

[38] Pezzato L, Brunelli K, Napolitani E, Magrini M, Dabalà M. Surface properties of AZ91 magnesium alloy after PEO treatment using molybdate salts and low current densities. Applied Surface Science. 2015;**357**:1031-1039. DOI: 10.1016/j.apsusc.2015.09.107

[39] Song YW, Shan DY, Han EH. High corrosion resistance of electroless composite plating coatings on AZ91D magnesium alloys. Electrochimica Acta. 2008;**53**:2135-2143. DOI: 10.1016/j.electacta.2007.09.026

[40] Brunelli K, Dabalá M, Calliani J, Magrini M. Effect of HCl pre-treatment on corrosion resistance of cerium-based conversion coatings on magnesium and magnesium alloys. Corrosion Science. 2005;**47**:989-1000. DOI: 10.1016/j.corsci.2004.06.016

[41] Hamlaoui Y, Pedraza F, Remazeilles C, Cohendoz S, Rébéré C, Tifouti L, et al. Cathodic electrodeposition of cerium-based oxides on carbon steel from concentrated cerium nitrate solutions: Part I. Electrochemical and analytical characterization. Materials Chemistry and Physics. 2009;**113**:650-657. DOI: 10.1016/j.matchemphys.2008.08.027

IntechOpen